

# Wavepacket Scattering Theory for the Coulomb Potential

Scott E. Hoffmann

*School of Mathematics and Physics  
University of Queensland  
Brisbane, QLD, 4072  
Australia\**

We treat the nonrelativistic quantum mechanical scattering of a wavepacket (for a single, charged, spinless particle) of well-resolved momentum incident on a fixed Coulomb potential. To implement this, we calculate the incoming and outgoing probability amplitudes for normalized state vectors on the basis of eigenvectors of total momentum magnitude and total angular momentum. We show that the method of partial wave analysis becomes applicable for this long range potential with the use of wavepackets. We find a relation between the finite probability and the differential cross section that is seen to hold sufficiently far from the singularity of the latter in the forward direction. The resulting differential cross section reduces to the familiar Rutherford form for scattering angles sufficiently far from the forward direction. We find that the interaction causes small time shifts in the detection probabilities. For our particular scattering geometry, we see, at low energies, a shadow zone of low probability for small angles around the forward direction, a phenomenon that cannot be predicted by the standard treatment.

## I. INTRODUCTION

The Coulomb potential is an exceptional case compared to shorter range potentials that fall off with radial distance,  $r$ , faster than  $1/r$  as  $r \rightarrow \infty$ . It has defied the use of conventional nonrelativistic scattering theory. As pointed out by Taylor [1], (i) the asymptotic condition is not applicable, (ii) the standard definitions of the scattering amplitude and the phase shifts are not applicable, and (iii) the partial wave series does not converge.

We present a treatment of the nonrelativistic scattering of a wavepacket from a potential using a basis of eigenvectors of total energy and total angular momentum. As such, our method is a combination of a wavepacket treatment and partial wave analysis. We demonstrate that all three of the above problems are solved with the use of a wavepacket treatment.

Other authors have used a wavepacket description of Coulomb scattering but have not combined that with partial wave analysis [2–4].

Boris *et al.* [5] used both a wavepacket treatment and partial wave analysis to give a spatial visualization of the scattering process. For an initial wavepacket state vector,  $|\psi(0)\rangle$ , they numerically calculated the amplitudes on the interacting basis vectors  $|k, l, m\rangle$ ,

$$\langle k, l, m | \psi(0) \rangle = \int d^3r \langle k, l, m | \mathbf{r} \rangle \langle \mathbf{r} | \psi(0) \rangle, \quad (1)$$

where the  $\langle \mathbf{r} | k, l, m \rangle$  are simply related to the energy and angular momentum eigenvectors of the full Coulomb Hamiltonian (by (13)). Then they plotted the position

probability density,  $|\psi(\mathbf{r}, t)|^2$ , where

$$\psi(\mathbf{r}, t) = \int_0^\infty dk \sum_{l=0}^\infty \sum_{m=-l}^l \langle \mathbf{r} | k, l, m \rangle \times e^{-ik^2 t/2m_0} \langle k, l, m | \psi(0) \rangle. \quad (2)$$

However, they did not extract the differential cross section or calculate time shifts. In Section VII we will compare our results with theirs.

Dollard [6] constructed a modified Møller operator for use with the long-range Coulomb potential. It is beyond the scope of the present work to provide comparisons between our method and his. Similarly, we merely mention the surface-integral formulation of scattering theory due to Kadyrov *et al.* [7, 8], which can also deal with the Coulomb potential.

Our method involves first finding the change of basis from free momentum eigenvectors,  $|\mathbf{k}; \text{free}\rangle$ , to free eigenvectors of the magnitude,  $k$ , of the momentum and the angular momentum quantum numbers  $l$  and  $m$ , denoted  $|k, l, m; \text{free}\rangle$ . These are simply related to eigenvectors of energy,  $E$ , and angular momentum by (13). This is done in Section II. Then we change the representation of a free initial wavepacket state vector from (11) to (12). This is not an exact result but the leading asymptotic approximation for a small fractional momentum spread. This is done in Section III.

Then we use the technique from partial wave analysis, as is done for short-range potentials, of adjusting the phase of this free wavefunction to give a representation of the incoming state vector. Our wavepacket method involves replacing a limit as time  $t \rightarrow -\infty$  with a limit as the momentum spread  $\sigma_p \rightarrow 0^+$ , to define the correspondence between free and incoming state vectors. This is done in Section IV. We will discuss the role of the logarithmic phase in (47) and determine that the correct treatment is to not compensate for this term.

---

\* scott.hoffmann@uqconnect.edu.au

We use the antiunitary time reversal operator to construct the outgoing state vectors. The measurement is modeled as the projection onto these outgoing state vectors.

In Section V we derive the connection, for Gaussian wavepackets, between finite probabilities and the differential cross section.

In Section VI we evaluate an integral over momentum magnitude  $k$  and numerically evaluate a sum over the angular momentum quantum number  $l$  to find the finite amplitude for the process. We explore the parameter space and present our results in Section VII.

In Section VIII we present an integral relation satisfied by our scattering probability that represents the conservation of total probability. We use this as a check on our results.

In Section IX we discuss the possibility of experimental measurement of some of the new phenomena we have predicted. Conclusions are presented in Section X.

For the nonrelativistic scattering of a spinless, charged particle in a static Coulomb field, the time-independent Schrödinger equation, with Hamiltonian in the  $\mathbf{x}$  representation

$$H = -\frac{1}{2m_0}\nabla^2 + \frac{Z_1 Z_2 \alpha}{|\mathbf{x}|}, \quad (3)$$

can be solved to find an energy eigenvector of the form

$$\psi(\mathbf{x}, p) = e^{ip|\mathbf{x}|\cos\theta} F(|\mathbf{x}|(1 - \cos\theta)), \quad (4)$$

as done in standard textbooks [9, 10], to then give the scattering amplitude

$$f(\theta, p) = -\frac{\eta}{2p \sin^2(\frac{\theta}{2})} \exp(-i\eta \ln(\sin^2(\frac{\theta}{2}))) + i2\sigma_0. \quad (5)$$

(Throughout this paper, we use Heaviside-Lorentz units, in which  $\hbar = c = \epsilon_0 = \mu_0 = 1$ .) The momentum magnitude,  $p$ , in terms of the energy,  $E$ , is

$$p = \sqrt{2m_0 E}. \quad (6)$$

The scattered wave is observed at the scattering angle  $\theta$  to the incident direction. The dimensionless quantity  $\eta$  is

$$\eta = Z_1 Z_2 \frac{\alpha}{\beta}, \quad (7)$$

where  $Z_1$  is the atomic number of the Coulomb field,  $Z_2$  is the atomic number of the incident particle, and

$$\beta = \frac{p}{m_0} \quad (8)$$

is the nonrelativistic form of the speed of the incoming particle of mass  $m_0$ . The quantity  $\alpha$  is the fine structure constant  $\alpha = e^2/4\pi \cong 1/137$ . The phase shifts for general  $l$  are defined by (48).

To make contact with experiment, the differential cross section is then given by

$$\frac{d\sigma}{d\Omega} = |f(\theta, p)|^2 \quad (9)$$

$$= \frac{Z_1^2 Z_2^2 \alpha^2 m_0^2}{4p^4 \sin^4(\frac{\theta}{2})}. \quad (10)$$

This is called the Rutherford cross section, since Rutherford used an entirely classical treatment of Coulomb scattering of point particles to obtain, remarkably, the same result as the later quantum calculation [11]. The experimental verification of this cross section formula is routinely done as a laboratory activity in undergraduate physics courses.

This scattering amplitude (5) is not an amplitude of the type for which the modulus-squared is a probability less than or equal to unity. For a start it is not dimensionless, instead having the dimensions of length. Furthermore it diverges in the forward direction,  $\theta = 0$ , for all momenta, and as  $p \rightarrow 0^+$  for all scattering angles.

One purpose of this paper is to find the relation between the scattering amplitude and what we will call the *finite amplitude* for this scattering process, which is simply the  $S$  matrix element between normalized wavepacket state vectors, and as such must be less than or equal to unity in magnitude. This relation, which we will derive for Gaussian wavepackets in Section V, will, in the case of more general interactions, only hold for scattering angles sufficiently far from the forward direction.

## II. THE CHANGE OF IMPROPER BASIS VECTORS

We first need to change the representation of a *free* wavepacket state vector, normalized to unity, from

$$|\psi; \text{free}\rangle = \int d^3k |\mathbf{k}; \text{free}\rangle \psi_{\text{free}}(\mathbf{k}) \quad (11)$$

to

$$|\psi; \text{free}\rangle = \int_0^\infty dk \sum_{l=0}^\infty \sum_{m=-l}^l |k, l, m; \text{free}\rangle \times \Psi_{\text{free}}(k, l, m), \quad (12)$$

where the  $|k, l, m; \text{free}\rangle$  are eigenvectors of the magnitude of momentum ( $k$ ) and angular momentum (the familiar quantum numbers  $l$  and  $m$  taking only integer values). Note that eigenvectors of energy ( $E$ ) and angular momentum are simply related to these by a change of normalization:

$$|E, j, m\rangle = |k, j, m\rangle \sqrt{\frac{m_0}{k}}. \quad (13)$$

We start with the improper basis vectors. The basis transformation is derived by Sakurai [12] and agrees

with our calculation. We want the  $|\mathbf{k}; \text{free}\rangle$  to have the orthonormality relation

$$\langle \mathbf{k}_1; \text{free} | \mathbf{k}_2; \text{free} \rangle = \delta^3(\mathbf{k}_1 - \mathbf{k}_2) \quad (14)$$

and the  $|k, l, m\rangle$  to obey the orthonormality relation

$$\langle k_1, l_1, m_1; \text{free} | k_2, l_2, m_2; \text{free} \rangle = \delta(k_1 - k_2) \delta_{l_1 l_2} \delta_{m_1 m_2}. \quad (15)$$

The result is

$$|\mathbf{k}; \text{free}\rangle = \sum_{l=0}^{\infty} \sum_{m=-l}^l |k, l, m; \text{free}\rangle \times Y_{lm}^*(\hat{\mathbf{k}}) \frac{1}{k}, \quad (16)$$

with  $k = |\mathbf{k}|$ , with a choice of global phase.

### III. BASIS TRANSFORMATION FOR A FREE WAVEPACKET STATE VECTOR

The free state vector that will be modified to become the incoming state vector is chosen as the Gaussian wavepacket Schrödinger picture state vector

$$|\mathbf{p}_i, \mathbf{R}_i; \sigma_p; \text{free}(0)\rangle = \int d^3k |\mathbf{k}; \text{free}\rangle e^{-i\mathbf{k} \cdot \mathbf{R}_i} \frac{e^{-|\mathbf{k} - \mathbf{p}_i|^2 / 4\sigma_p^2}}{(2\pi\sigma_p^2)^{3/4}}. \quad (17)$$

The average momentum is

$$\mathbf{p}_i = p \hat{\mathbf{z}}. \quad (18)$$

The standard deviation of momentum in all directions is  $\sigma_p$ . We are going to choose a very well resolved momentum,

$$\epsilon = \frac{\sigma_p}{p} \ll 1, \quad (19)$$

and we will only need the leading asymptotic approximation to the wavefunction  $\Psi_{\text{free}}(k, j, m)$  in powers of  $\sqrt{\epsilon}$ , as will be explained shortly. The average position at  $t = 0$  is

$$\mathbf{R}_i = -R \hat{\mathbf{z}}. \quad (20)$$

The standard deviation of position in all directions at  $t = 0$  is  $\sigma_x$  with

$$\sigma_x \sigma_p = \frac{1}{2}. \quad (21)$$

The distance,  $R$ , from the center of the Coulomb potential at  $t = 0$  must be large so that the corresponding *interacting* state vector is effectively free at that time, and so that we can apply an approximation in Section V. However there must be a limit on the size of  $R$ . In our

scattering geometry, over the time of the experiment, the incoming wavepacket will traverse a distance of about  $2R$ . We demand that the *spreading* of the wavepacket be negligible over this time. The nonrelativistic law for spreading of Gaussian wavepackets is [10]

$$\sigma_x(t) = \sqrt{\sigma_x^2 + \left(\frac{\sigma_p}{p}\right)^2 (\beta t)^2}, \quad (22)$$

where  $t$  is the time measured from minimality. We see that spreading becomes significant for

$$\beta t \sim \frac{p}{\sigma_p} \sigma_x. \quad (23)$$

If we instead choose

$$R = \sqrt{\frac{p}{\sigma_p}} \sigma_x = \frac{1}{\sqrt{\epsilon}} \sigma_x, \quad (24)$$

we will still have a very large initial distance for  $\epsilon \ll 1$ , much larger than the initial spread, but wavepacket spreading will be negligible over the time of the experiment.

Now we transform the wavefunction. Using (11), (12) and (16), we find the transformation

$$\Psi_{\text{free}}(k, l, m) = k \int_0^\pi \sin \theta_k d\theta_k \int_0^{2\pi} d\varphi_k Y_{lm}^*(\theta_k, \varphi_k) \psi_{\text{free}}(\mathbf{k}), \quad (25)$$

again with  $k = |\mathbf{k}|$  and with  $\hat{\mathbf{k}} = (\theta_k, \varphi_k)$ .

The spherical harmonic is

$$Y_{lm}^*(\hat{\mathbf{k}}) = \sqrt{\frac{2l+1}{4\pi}} e^{-im\varphi_k} d_{m0}^l(\theta_k), \quad (26)$$

where

$$d_{m_1 m_2}^l(\theta_k) = \langle l, m_1 | e^{-i\theta_k J_y} | l, m_2 \rangle \quad (27)$$

are Wigner rotation matrices [9].

The  $\varphi_k$  integral is simply

$$\int_0^{2\pi} d\varphi_k e^{-im\varphi_k} = 2\pi \delta_{m0}. \quad (28)$$

We have

$$|\mathbf{k} - \mathbf{p}_i|^2 = (k - p)^2 + 2kp(1 - \cos \theta_k). \quad (29)$$

To eventually calculate an amplitude for the scattering process, we will be evaluating an integral over  $k$  in which a factor  $g(k)^2$  will appear, where

$$g(k) = e^{-(k-p)^2 / 4\sigma_p^2}. \quad (30)$$

This factor is sharply peaked in  $k$  with a width of  $\mathcal{O}(\sigma_p)$ . We will repeatedly find integrands similarly dominated by narrow factors, including the integral over  $\theta_k$ , which contains the factor

$$h(\theta_k) = e^{-kp(1 - \cos \theta_k) / 2\sigma_p^2}. \quad (31)$$

This function is sharply peaked at  $\theta_k = 0$  with a width of order  $\sigma_p/p$ . We need to find the leading approximation to such integrals for  $\sigma_p/p \ll 1$ , along with an estimate of the remainder. We use the technique of expanding the exponents (and more slowly varying factors) in powers of  $k - p$ , treating this as a quantity of  $\mathcal{O}(\sigma_p)$ , and in powers of  $\theta_k$ , treating this as a quantity of  $\mathcal{O}(\sigma_p/p)$ . We then evaluate the integrals to lowest order and estimate that the fractional remainder is no larger than  $\mathcal{O}(\sqrt{\epsilon})$ , uniform in the remaining variables.

With this method, we find

$$\frac{kp}{\sigma_p^2}(1 - \cos \theta_k) = \frac{p^2 \theta_k^2}{2\sigma_p^2} + \mathcal{O}(\epsilon). \quad (32)$$

Similarly, we find that we can replace

$$-i\mathbf{k} \cdot \mathbf{R}_i = +ikR + \mathcal{O}(\sqrt{\epsilon}) \quad (33)$$

using our scheme to avoid wavepacket spreading. Here  $k$  cannot be replaced by  $p$ .

With these approximations, we need to evaluate the integral (after using  $\sin \theta_k = \theta_k(1 + \mathcal{O}(\epsilon^2))$ )

$$I(l, \epsilon) = \int_0^\pi \theta_k d\theta_k e^{-p^2 \theta_k^2 / 4\sigma_p^2} d_{00}^l(\theta_k). \quad (34)$$

We cannot use a power series in  $\theta_k$  for the Wigner rotation matrix,  $d_{00}^l(\theta_k)$ , as for large  $l$  it will have rapid variation on the region  $0 \leq \theta_k \leq \epsilon$ . Instead, we use an approximation [13] valid for small  $\theta$ , uniform in  $l$ :

$$d_{00}^l(\theta_k) = J_0\left(\sqrt{l(l+1) + \frac{1}{3}}\theta_k\right) \times (1 + \mathcal{O}(\theta_k^2)) \quad (35)$$

(This result has been checked numerically.) Then the integral evaluates to [14]

$$I(l, \epsilon) = \frac{2\sigma_p^2}{p^2} \exp(-\sigma_p^2(l + \frac{1}{2})^2/p^2) \times (1 + \mathcal{O}(\epsilon^2)). \quad (36)$$

Finally the leading asymptotic approximation to the  $k, j, m$  representation of the free state vector is given by the normalized wavefunction

$$\Psi_{\text{free}}(k, j, m | \mathbf{p}_i, \mathbf{R}_i; \sigma_p) = \delta_{m0} e^{ikR} \frac{e^{-(k-p)^2/4\sigma_p^2}}{(2\pi\sigma_p^2)^{\frac{1}{4}}} \frac{\sqrt{l + \frac{1}{2}} e^{-\sigma_p^2(l + \frac{1}{2})^2/p^2}}{p/2\sigma_p}. \quad (37)$$

Note that a narrow distribution in angle produces a wide distribution in angular momentum.

#### IV. CONSTRUCTION OF THE INCOMING AND OUTGOING STATE VECTORS

We will be considering a range of different incident momentum magnitudes,  $p$ . In each case, we require that

the fractional momentum spread,  $\sigma_p(p)/p$ , be small. The simplest scheme is to make this quantity a constant independent of momentum:

$$\frac{\sigma_p(p)}{p} \equiv \epsilon \ll 1. \quad (38)$$

It will also become necessary to impose a lower limit on momentum for a given  $\epsilon$ , thereby imposing an upper limit on the quantity  $|\eta(p)|$  in (61) below. Note that we can still consider arbitrarily small momentum magnitudes, but only by decreasing  $\epsilon$ . In our numerical calculations, we will use  $\epsilon = 0.001$ , which gives  $\sqrt{\epsilon} \cong 0.032$ , sufficiently small for our purposes.

In scattering theory [1, 15], we define two mappings from free state vectors to interacting state vectors, provided by the Møller operators  $\Omega^{(+)}$  and  $\Omega^{(-)}$ . It is supposed that for an arbitrary free state vector, an interacting state vector can always be constructed that behaves in an essentially free manner at very early times, with properties matching those of the free state vector at those early times. We say that this interacting state vector is the incoming state vector corresponding to that free state vector, and write

$$|\text{incoming}\rangle = \Omega^{(+)}|\text{free}\rangle. \quad (39)$$

It should be clear that this correspondence only makes physical sense for wavepacket state vectors, where there is a position distribution that may be localized far from the scattering center at very early times. However, once it is constructed, the Møller operator will have matrix elements between plane-wave improper state vectors.

The other Møller operator,  $\Omega^{(-)}$ , maps from free to outgoing state vectors, such that the latter are essentially free as  $t \rightarrow +\infty$ .

The incoming correspondence is defined by requiring

$$\lim_{t \rightarrow -\infty} \int d^3r |\psi_{\text{in}}(\mathbf{r}, t) - \psi_{\text{free}}(\mathbf{r}, t)|^2 = 0. \quad (40)$$

In contrast, in our method we only need to find the free to interacting correspondence for two particular sets of state vectors, namely

$$|\mathbf{p}_i, \mathbf{R}_i, \sigma_p; \text{in}\rangle = \Omega^{(+)}|\mathbf{p}_i, \mathbf{R}_i, \sigma_p; \text{free}\rangle \quad (41)$$

and

$$|\mathbf{p}_f, \mathbf{R}_f, \sigma_p; \text{out}\rangle = \Omega^{(-)}|\mathbf{p}_f, \mathbf{R}_f, \sigma_p; \text{free}\rangle, \quad (42)$$

where the latter will be defined below. We consider the incoming case first.

Since, for small  $\epsilon$ , the free wavepacket is already localized far from the scattering centre at  $t = 0$ , we argue that the interacting state vector should be essentially free at  $t = 0$ , not just as  $t \rightarrow -\infty$ . This leads to two constraints. The probability distribution in  $k, l$  and  $m$  is independent of time for the interacting system, so it must be equal to its value as  $t \rightarrow -\infty$ , when we argue that it must take

its free value exactly (for negligible bound state content in the attractive case). Hence

$$|\Psi_{\text{in}}(k, l, m)|^2 = |\Psi_{\text{free}}(k, l, m)|^2. \quad (43)$$

(The modifications imposed by the logarithmic phase in (47) will not negate this argument.) In practice we equate  $|\Psi_{\text{in}}(k, l, m)|^2$  to the leading asymptotic approximation as  $\epsilon \rightarrow 0^+$  of  $|\Psi_{\text{free}}(k, l, m)|^2$ , given by (37), with the knowledge that the error is negligible for the value of  $\epsilon$  that we consider.

Then the position probability density at  $t = 0$  must approach its free form in the limit as  $\epsilon \rightarrow 0^+$ ,

$$\lim_{\epsilon \rightarrow 0^+} \{|\psi_{\text{in}}(\mathbf{r}, 0)|^2 - |\psi_{\text{free}}(\mathbf{r}, 0)|^2\} = 0. \quad (44)$$

(This argument will need to be modified when taking into account the effect of the logarithmic phase.) We will see below how simple it is to apply this limit in practice. Compared to (40), there is no need to evolve the wavefunctions towards infinite times.

The first of these equations implies that the interacting and free  $k, l, m$  wavefunctions can only differ by a phase factor

$$\Psi_{\text{in}}(k, l, m) = e^{i\chi_l(k)} \Psi_{\text{free}}(k, l, m). \quad (45)$$

The fact that  $\delta_l(k)$  is independent of  $m$  follows from the extra physical requirement that rotations commute with the Møller operators. (The phase factor  $\exp(ikR)$  from  $\Psi_{\text{free}}(k, j, m | \mathbf{p}_i, \mathbf{R}_i; \sigma_p)$  is physically relevant and will be retained.)

Now we impose the constraint (44) on the incoming position probability amplitude,

$$\begin{aligned} \psi_{\text{in}}(\mathbf{r}, 0) = & \int_0^\infty dk \sum_{l=0}^\infty \sum_{m=-l}^l \langle \mathbf{r} | k, l, m \rangle e^{i\chi_l(k)} e^{ikR} |\Psi_{\text{free}}(k, l, m)|. \end{aligned} \quad (46)$$

It is clear that for large  $R$  we can use an approximation for large  $r$  if the incoming probability density is to have a similar form to the free density. We use the known solutions [9] (with continuum normalization similar to (15)) with asymptotic form as  $r = |\mathbf{r}| \rightarrow \infty$ ,

$$\begin{aligned} \langle \mathbf{r} | k, l, m \rangle \sim & \sqrt{\frac{2}{\pi}} Y_{lm}(\hat{\mathbf{r}}) \frac{1}{r} \times \\ & \times \sin(kr - \eta(k) \ln(2kr) - l\frac{\pi}{2} + \sigma_l(k)), \end{aligned} \quad (47)$$

where the Coulomb phase shifts,  $\sigma_l$ , are defined implicitly by

$$e^{i2\sigma_l(k)} = \frac{\Gamma(l+1+i\eta(k))}{\Gamma(l+1-i\eta(k))}. \quad (48)$$

In contrast, the free spherical waves have the asymptotic form

$$\langle \mathbf{r} | k, l, m; \text{free} \rangle \sim \sqrt{\frac{2}{\pi}} Y_{lm}(\hat{\mathbf{r}}) \frac{1}{r} \sin(kr - l\frac{\pi}{2}) \quad (49)$$

and the free position probability amplitude is

$$\begin{aligned} \psi_{\text{free}}(\mathbf{r}, 0) = & \int_0^\infty dk \sum_{l=0}^\infty \sum_{m=-l}^l \langle \mathbf{r} | k, l, m; \text{free} \rangle e^{ikR} |\Psi_{\text{free}}(k, l, m)|, \end{aligned} \quad (50)$$

which evaluates to

$$\psi_{\text{free}}(\mathbf{r}, 0) = e^{i\mathbf{p}_i \cdot (\mathbf{r} - \mathbf{R}_i)} \frac{e^{-|\mathbf{r} - \mathbf{R}_i|^2 / 4\sigma_x^2}}{(2\pi\sigma_x^2)^{3/4}}. \quad (51)$$

Note that for shorter range potentials, there will be different phase shifts instead of  $\sigma_l(k)$  and the logarithmic phase term  $-\eta(k) \ln(2kr)$  will be absent.

In

$$\sin \varphi = \frac{1}{2i} (e^{+i\varphi} - e^{-i\varphi}) \quad (52)$$

with

$$\varphi = kr - \eta(k) \ln(2kr) - l\frac{\pi}{2} + \sigma_l(k), \quad (53)$$

only the integral over  $k$  containing  $\exp(-i\varphi) \exp(+ikR)$  will be significant on  $r \geq 0$ . So the relevant phase to consider is

$$\Phi(k, r) = kR - kr + \eta(k) \ln(2kr) - \sigma_l(k) + \chi_l(k), \quad (54)$$

in comparison with

$$\Phi_{\text{free}}(k, r) = kR - kr, \quad (55)$$

which leads to a peak probability density at  $r = R$ .

We would like to be able to choose  $\delta_l(k)$  to cancel both the Coulomb phase shifts and the logarithmic phase. This is not possible, since the latter is a function of  $r$  and  $\chi_l(k)$  cannot depend on  $r$ . Instead, we choose

$$\chi_l(k) = \sigma_l(k) \quad (56)$$

and investigate the physical effects of the logarithmic phase.

We expand in powers of  $k - p$ :

$$\begin{aligned} \eta(k) \ln(2kr) = & \eta(p) \ln(2pr) \\ & - \frac{(k-p)}{p} \eta(p) (\ln(2pr) - 1) + \dots \end{aligned} \quad (57)$$

The remainder is found to be negligible for  $r = R$  and  $|\eta(p)| = 844$  (see (61) below).

The first term in (57) is independent of  $k$  so merely contributes an  $r$ -dependent phase factor to the position wavefunction. The second term produces a spatial shift of the peak of the position wavefunction away from its free value of  $R$ . To see this, we note that  $\Phi(k, r)$  is stationary in  $k$  at the peak,  $k = p$ , for  $r = \bar{r}$  satisfying

$$R - \bar{r} - \frac{\eta(p)}{p}(\ln(2p\bar{r}) - 1) = 0. \quad (58)$$

Inverting for large  $R$  gives the asymptotic behaviour

$$\bar{r}(R) \sim R - \Delta(R), \quad (59)$$

with

$$\Delta(R) = \frac{\eta(p)}{p}(\ln(2pR) - 1). \quad (60)$$

(It will be easily seen that the same result will hold for the outgoing state vectors.)

We suppose that  $|\Delta(R)|$  could be as large as  $R/2$  without affecting the negligibility of wavepacket spreading or the requirement that the mean initial radial distance of the wavepacket grow as  $\epsilon^{-3/2}$  for given momentum. This leads to

$$|\eta(p)| \leq \frac{1}{4\epsilon^{3/2}|\frac{3}{2}\ln\frac{1}{\epsilon} - 1|} = 844 \quad (61)$$

for  $\epsilon = 0.001$ .

So, with our choice of phase (56) to define the incoming state vector corresponding to a free state at average radial position  $R$ , the actual average position of the incoming state vector is at radius  $R - \Delta(R)$ . It is clear that the incoming state can never be considered entirely free, since evolution over short times will always give

$$U(t)|\mathbf{p}_i, \mathbf{R}_i, \sigma_p; \text{in}\rangle \neq |\mathbf{p}_i, \mathbf{R}_i + \frac{\mathbf{p}_i}{m_0}t, \sigma_p; \text{in}\rangle. \quad (62)$$

We argue that this is the correct physical behaviour for a particle in a Coulomb field because very similar behaviour is seen in the classical case at large distances from the origin. A straightforward calculation of the classical trajectories for a head-on collision shows that if free motion is defined as

$$R(t) = R_0 + \frac{p}{m_0}t, \quad (63)$$

where  $p$  is the finite limit of momentum magnitude far from the origin, then the actual position of the particle has the asymptotic form for large  $R$

$$\bar{r}(R) \sim R - \frac{\eta(p)}{p}(\ln(2pR) - \ln\eta), \quad (64)$$

in asymptotic agreement with the quantum calculation as  $R \rightarrow \infty$ . The sign of this effect can be understood. For a repulsive interaction ( $\eta > 0$ ) the outgoing particle is constantly being accelerated, but by decreasing amounts

as it moves further from the origin. So its speed is always less than the asymptotic limit. Integrating shows that its radial position is always less than the leading asymptotic behaviour (which is linear in time).

A longitudinal spatial shift will not change the  $k, l, m$  probability density, so the conclusion (43) stands. We now see how the constraint (44) must be modified to

$$\lim_{\epsilon \rightarrow 0^+} \{|\psi_{\text{in}}(\mathbf{r}, 0)|^2 - |\psi_{\text{free}}(\mathbf{r} - \Delta(R)\hat{\mathbf{p}}_i, 0)|^2\} = 0. \quad (65)$$

In practice we define a dimensionless variable  $\zeta$ , scaled by the  $\epsilon$ -dependent width  $\sigma_x$ , and write

$$\rho_{\text{free}}(\zeta; \epsilon) = \sigma_x^3 |\psi_{\text{free}}(\sigma_x \zeta - R\hat{\mathbf{p}}_i, 0)|^2 \quad (66)$$

and

$$\rho_{\text{in}}(\zeta; \epsilon) = \sigma_x^3 |\psi_{\text{in}}(\sigma_x \zeta - R\hat{\mathbf{p}}_i + \Delta(R)\hat{\mathbf{p}}_i, 0)|^2, \quad (67)$$

both of which peak at  $\zeta = 0$  and are expected to have finite limits as  $\epsilon \rightarrow 0^+$ . Note that  $\epsilon$  is a physical parameter of the model that always takes a nonzero value, so instead of a limit we actually require

$$\rho_{\text{in}}(\zeta; \epsilon) = \rho_{\text{free}}(\zeta; \epsilon) + \mathcal{R}(\epsilon) \quad (68)$$

$$= \frac{e^{-|\zeta|^2/2}}{(2\pi)^{3/2}} + \mathcal{R}(\epsilon) \quad (69)$$

with the remainder  $\mathcal{R}(\epsilon)$  negligible for the small  $\epsilon$  that we consider, uniformly in  $\zeta$  and  $p$ . Clearly this result is satisfied in our case.

Our final result for the wavefunction of the incoming state vector is

$$\Psi_{\text{in}}(k, l, m | \mathbf{p}_i, \mathbf{R}_i; \sigma_p) = e^{+i\sigma_l(k)} e^{+ikR} \delta_{m0} \times |\Psi_{\text{free}}(k, l, 0 | \mathbf{p}_i, \mathbf{R}_i; \sigma_p)|. \quad (70)$$

We use the antiunitary time reversal operator,  $A(\mathcal{T})$ , to construct the outgoing state vector as the time reversal of an incoming state vector is an outgoing state vector. It can be shown [10] that the transformation law of the interacting eigenvectors is

$$A(\mathcal{T}) |k, l, m\rangle = (-)^{l+m} |k, l, -m\rangle. \quad (71)$$

Starting with

$$|\mathbf{p}_i, \mathbf{R}_i, \sigma_p; \text{in}\rangle = \int_0^\infty dk \sum_{l=0}^\infty |k, l, 0\rangle \Psi_{\text{in}}(k, l, 0) \quad (72)$$

and applying a time reversal, a rotation by  $\pi$  about the  $y$  axis and then a further rotation by  $\theta$  about the  $y$  axis gives

$$|\mathbf{p}_f, \mathbf{R}_f, \sigma_p; \text{out}\rangle \equiv U(R_y(\pi + \theta))A(\mathcal{T}) |\mathbf{p}_i, \mathbf{R}_i, \sigma_p; \text{in}\rangle, \quad (73)$$

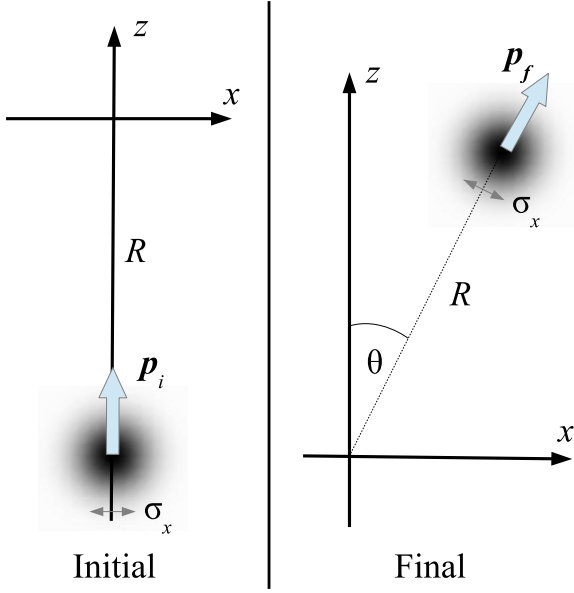


Figure 1. Scattering geometry.

so

$$\begin{aligned} & |\mathbf{p}_f, \mathbf{R}_f, \sigma_p; \text{out}\rangle \\ &= \int_0^\infty dk \sum_{l=0}^\infty \sum_{m=-l}^l |k, l, m\rangle d_{m0}^l(\theta) \Psi_{\text{in}}^*(k, l, 0). \end{aligned} \quad (74)$$

We have chosen

$$\mathbf{R}_f = R(\sin \theta, 0, \cos \theta). \quad (75)$$

So

$$\begin{aligned} \Psi_{\text{out}}(k, l, m | \mathbf{p}_f, \mathbf{R}_f; \sigma_p) &= e^{-i\sigma_l(k)} e^{-ikR} d_{m0}^l(\theta) \times \\ &\times |\Psi_{\text{free}}(k, l, 0 | \mathbf{p}_i, \mathbf{R}_i; \sigma_p)|. \end{aligned} \quad (76)$$

Calculation of  $\psi_{\text{out}}(r, 0)$  involves the  $\exp(+i\varphi)$  factor and arrives at the same result (59,60) for the shift due to the logarithmic phase term.

Our scattering geometry is shown in Figure 2.

## V. CONNECTION BETWEEN FINITE AMPLITUDES, SCATTERING AMPLITUDES AND $S$ MATRIX ELEMENTS

The quantity that we call a finite amplitude, with  $|i\rangle$  an incoming state vector and  $|f\rangle$  an outgoing state vector, is clearly an  $S$  matrix element between normalized wavepacket state vectors

$$\begin{aligned} & \langle f | e^{-iHt} | i \rangle = \\ & \langle \mathbf{p}_f, \mathbf{R}_f, \sigma_p; \text{free}(0) | S | \mathbf{p}_i, \mathbf{R}_i, \sigma_p; \text{free}(t) \rangle. \end{aligned} \quad (77)$$

We used

$$e^{-iHt} \Omega^{(+)} | \text{free} \rangle = \Omega^{(+)} e^{-iH_0 t} | \text{free} \rangle, \quad (78)$$

which follows from the fact that the Moller operator simply changes basis vectors from  $|k, l, m; \text{free}\rangle$  to  $|k, l, m\rangle$  and multiplies by a phase factor, and the definition of the  $S$  matrix [15]

$$S = \Omega^{(-)\dagger} \Omega^{(+)}. \quad (79)$$

For state vectors normalized to unity, the Schwartz inequality [9] guarantees

$$|\langle f | e^{-iHt} | i \rangle|^2 \leq 1. \quad (80)$$

$S$  matrix elements between momentum eigenvectors are related to scattering amplitudes by (see Wichmann [16] for a derivation using wavepackets)

$$\begin{aligned} \langle \mathbf{k}_f; \text{free} | S | \mathbf{k}_i; \text{free} \rangle &= \delta^3(\mathbf{k}_f - \mathbf{k}_i) + \\ &+ \frac{i}{2\pi k_i} \delta(k_f - k_i) f(\theta, k_i). \end{aligned} \quad (81)$$

With  $S = 1 + iT$ , we can find the  $T$  matrix element between our Gaussian wavepacket state vectors, by approximating the integrals for  $\sigma_p/p \ll 1$ , to give

$$\begin{aligned} \langle \mathbf{p}_f, \mathbf{0}; \sigma_p; \text{free} | T | \mathbf{p}_i, \mathbf{0}; \sigma_p; \text{free} \rangle &= \\ \frac{4\sigma_p^2}{p} f(\theta, p) (1 + \mathcal{O}(\epsilon)). \end{aligned} \quad (82)$$

(The average positions of the wavepackets are not important to this calculation, but will be relevant later.)

Then we find the differential cross section to be (using (9)), for  $\epsilon \ll 1$ ,

$$\begin{aligned} \frac{d\sigma}{d\Omega} &= \\ \frac{p^2}{16\sigma_p^4} |\langle \mathbf{p}_f, \mathbf{0}; \sigma_p; \text{free} | T | \mathbf{p}_i, \mathbf{0}; \sigma_p; \text{free} \rangle|^2. \end{aligned} \quad (83)$$

If we only consider directions sufficiently far away from the forward direction, as will be discussed later, we can write

$$\begin{aligned} \frac{d\sigma}{d\Omega} &= \\ \frac{p^2}{16\sigma_p^4} |\langle \mathbf{p}_f, \mathbf{0}; \sigma_p; \text{free} | S | \mathbf{p}_i, \mathbf{0}; \sigma_p; \text{free} \rangle|^2, \end{aligned} \quad (84)$$

or

$$\frac{d\sigma}{d\Omega} = \frac{p^2}{16\sigma_p^4} |\langle f | e^{-iHt} | i \rangle|^2. \quad (85)$$

There is a simple way to see how the powers of  $\sigma_p$  and  $p$  arise. The area of the incoming wavepacket perpendicular to the average momentum direction scales as

$$A \sim \sigma_x^2 \sim \frac{1}{\sigma_p^2}. \quad (86)$$

The final state solid angle element scales as

$$\Delta\Omega \sim \left(\frac{\sigma_p}{p}\right)^2. \quad (87)$$

Then the probability of the event is

$$P \sim \frac{d\sigma}{A} \quad (88)$$

$$= \frac{d\sigma}{d\Omega} \Delta\Omega \frac{1}{A}, \quad (89)$$

so

$$\frac{d\sigma}{d\Omega} \sim \frac{p^2}{\sigma_p^4} P. \quad (90)$$

## VI. EVALUATION OF THE FINITE AMPLITUDE AND EXTRACTION OF THE SCATTERING AMPLITUDE

We now have the finite amplitude, using (70,76) and  $d_{00}^l(\theta) = P_l(\cos\theta)$ , a Legendre polynomial,

$$\begin{aligned} \langle f | e^{-iHt} | i \rangle = \\ \int_0^\infty dk \sum_{l=0}^\infty |\Psi_{\text{free}}(k, l)|^2 e^{i\varphi(k, l)} P_l(\cos\theta) \times \\ \times (1 + \mathcal{O}(\sqrt{\epsilon})), \end{aligned} \quad (91)$$

where the phases are

$$\varphi(k, l) = 2kR - \frac{k^2 t}{2m_0} + 2\sigma_l(k). \quad (92)$$

Of course time evolution takes its simplest representation in a basis of total energy eigenvectors.

The time evolution phase factor is

$$e^{-ik^2 t/2m_e} = e^{-ip^2 t/2m_0} e^{-i\beta t(k-p)} (1 + \mathcal{O}(\sqrt{\epsilon})), \quad (93)$$

with the speed  $\beta$  given by (8).

We also expand the Coulomb phase shifts in powers of  $k - p$ :

$$\sigma_l(k) = \sigma_l(p) + (k - p) \frac{\partial \sigma_l(p)}{\partial k} + \mathcal{R}(k, l). \quad (94)$$

A numerical investigation shows that the remainder,  $\mathcal{R}(k, l)$ , is negligible on our parameter space.

So we can find the leading approximation to the  $k$  integral for small  $\epsilon$ ,

$$\int_0^\infty dk e^{-(k-p)^2/2\sigma_p^2} e^{-i(k-p)\Delta_l(t)} \sim \sqrt{2\pi\sigma_p^2} e^{-\Delta_l^2(t)/8\sigma_x^2} \quad (95)$$

(with error  $\exp(-C/\epsilon^2)$  from extending the lower limit of the integral to  $-\infty$ ), to give

$$\begin{aligned} |\langle f | e^{-iHt} | i \rangle| = \\ \left| \sum_{l=0}^\infty \frac{(l + \frac{1}{2}) e^{-2\sigma_p^2(l + \frac{1}{2})^2/p^2}}{(p/2\sigma_p)^2} \times \right. \\ \left. \times e^{-\Delta_l^2(t)/8\sigma_x^2} e^{i2\sigma_l(p)} P_l(\cos\theta) \right| \times \\ \times (1 + \mathcal{O}(\sqrt{\epsilon})), \end{aligned} \quad (96)$$

with

$$\Delta_l(t) = \beta t - 2R - 2 \frac{\partial \sigma_l(p)}{\partial k}. \quad (97)$$

Taking into account the spatial shifts caused by the logarithmic phase, the time it would take a free particle to start at radius  $R - \eta(p)(\ln(2pR) - 1)/p$ , be deflected at the origin without time shift and finish at radius  $R - \eta(p)(\ln(2pR) - 1)/p$  would be  $T_{\text{free}}$  with

$$\beta T_{\text{free}} = 2R - 2 \frac{\eta(p)}{p} (\ln(2pR) - 1). \quad (98)$$

For the actual interacting evolution, we define the spatial shift ( $\beta$  times the time delay) as a function of time,  $t$ , in units of  $\sigma_x$ , as

$$\delta(t) \equiv \frac{\beta t - \beta T_{\text{free}}}{\sigma_x} \quad (99)$$

$$= \frac{\beta t - 2R + 2\eta(p)(\ln(2pR) - 1)/p}{\sigma_x}. \quad (100)$$

Then the Gaussian time-dependent factor becomes

$$e^{-\Delta_l^2(t)/8\sigma_x^2} = e^{-(\delta(t) - \xi_l(p))^2/8} \quad (101)$$

with

$$\xi_l(p) \equiv 4\epsilon\eta(p)\{\ln(2pR) - 1 - \frac{\partial \sigma_l[\eta(p)]}{\partial \eta}\}. \quad (102)$$

We used

$$\frac{\partial \sigma_l(p)}{\partial k} = -\frac{\eta(p)}{p} \frac{\partial \sigma_l[\eta(p)]}{\partial \eta}. \quad (103)$$

The form on the RHS is more advantageous for computation.

Now we numerically evaluate the series in

$$\begin{aligned} |\langle f | e^{-iHT} | i \rangle|^2 = \\ 16\epsilon^4 \left| \sum_{l=0}^\infty \left(l + \frac{1}{2}\right) e^{-2\epsilon^2(l + \frac{1}{2})^2} \times \right. \\ \left. \times e^{-(\delta - \xi_l(p))^2/8} e^{i2\sigma_l(p)} P_l(\cos\theta) \right|^2 \end{aligned} \quad (104)$$

to find the probability of the process. In practice we scan in  $\delta$  to find the peak.

Note that this formula (104) can be used for any non-Coulombic central potential with the replacements

$$\sigma_l(p) \rightarrow \delta_l(p), \quad (105)$$

$$\xi_l(p) \rightarrow \frac{2}{\sigma_x} \frac{\partial \delta_l(p)}{\partial k}, \quad (106)$$

where  $\delta_l(k)$  are the phase shifts for that potential and there are no logarithmic phase contributions to  $\xi_l(p)$ .



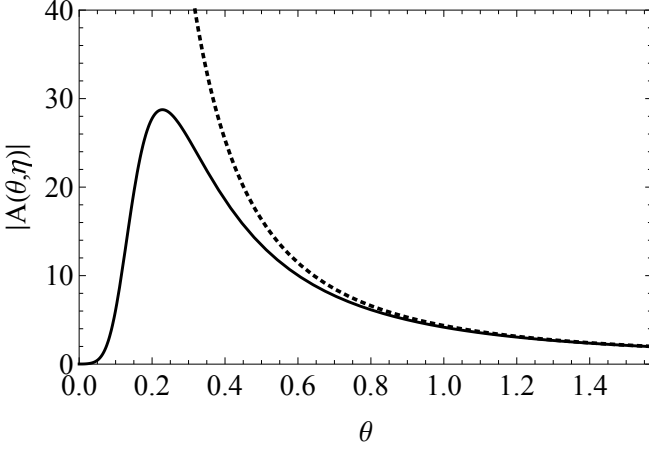


Figure 2. The angular function  $|A(\theta, \eta)|$  (solid) compared with  $1/\sin^2(\theta/2)$  (dotted) for  $\eta = 8$ ,  $\epsilon = 0.01$ .

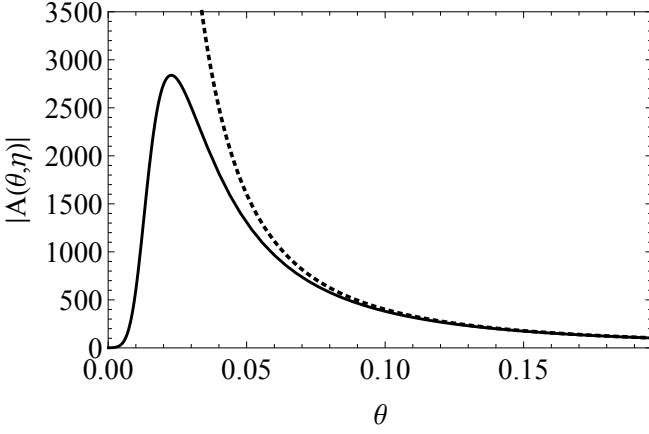


Figure 3. The angular function  $|A(\theta, \eta)|$  (solid) compared with  $1/\sin^2(\theta/2)$  (dotted) for  $\eta = 8$ ,  $\epsilon = 0.001$ .

## VII. RESULTS

As a first investigation, we leave out the factor  $\exp(-(\delta - \xi_l(p))^2/8)$ . From (5), (84) and (104), we expect that the magnitude of the quantity

$$A(\theta, \eta) = \frac{1}{\eta} \sum_{l=0}^{\infty} (2l+1) e^{-2\epsilon^2(l+\frac{1}{2})^2} e^{i2\sigma_l(p)} P_l(\cos \theta) \quad (107)$$

will converge to  $1/\sin^2(\theta/2)$ , independent of  $p$  and  $\sigma_p$ , sufficiently far from  $\theta = 0$ .

We first set  $\eta = 8$  and  $\epsilon = 0.01$  (a choice allowed by (61)). The results are shown in Figure 2. We see that the function is everywhere finite, and deviates from the Rutherford form only at low angles.

For comparison, we use the same value for  $\eta$  ( $\eta = 8$ ) and decrease  $\epsilon$  to 0.001, giving the result shown in Figure 3.

We see the Rutherford form holding to lower angles for

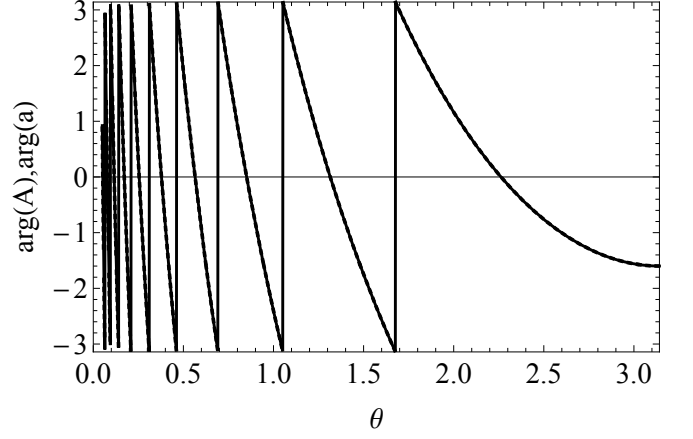


Figure 4. Comparison of  $\arg(A(\theta, \eta))$  (solid) and  $\arg(a(\theta, \eta))$  (dotted) for  $\eta = 10$ ,  $\epsilon = 0.001$ .

a smaller value of the momentum resolution parameter  $\epsilon$ .

We verified that  $|A(\theta, \eta)| \sin^2(\theta/2)$  was numerically independent of  $\eta$  and equal to unity for  $\epsilon = 0.001$  and  $\eta \leq 53.4$  and a selection of angles,  $\theta$ , away from the forward scattering region. This confirms the correct momentum dependence of the differential cross section (10).

The successful prediction of the Rutherford formula suggests that the result is insensitive to the shape of the wavepackets, which enters in (25) and (82). Investigation of this will await further work.

We plot the argument of the complex function  $A(\theta)$  compared with the argument of

$$a(\theta, \eta) = -\frac{i}{\sin^2(\frac{\theta}{2})} \exp(-i\eta \ln(\sin^2(\frac{\theta}{2}))) + i2\sigma_0, \quad (108)$$

in Figure 5.

It is remarkable to note that while the unregulated sum (we write  $\sigma_l[\eta]$  instead of  $\sigma_l(p)$ )

$$S_{\text{unreg}}(\theta, \eta) = \sum_{l=0}^{\infty} (2l+1) e^{i2\sigma_l[\eta]} P_l(\cos \theta) \quad (109)$$

does not converge for any value of  $\theta$  or  $\eta$ , the regulated sums

$$S_{\text{reg}}(\theta, \eta, \epsilon) = \sum_{l=0}^{\infty} (2l+1) e^{-2\epsilon^2(l+\frac{1}{2})^2} e^{i2\sigma_l[\eta]} P_l(\cos \theta) \quad (110)$$

are approaching a limit *independent of*  $\epsilon$  as  $\epsilon \rightarrow 0^+$  and  $0 < \theta \leq \pi$ .

Like the unregulated sum for the Dirac delta function,  $\delta(\cos \theta - 1)$ ,

$$S_{\text{unreg}}(\theta) = \sum_{l=0}^{\infty} \frac{2l+1}{2} P_l(\cos \theta) P_l(1) \quad (111)$$

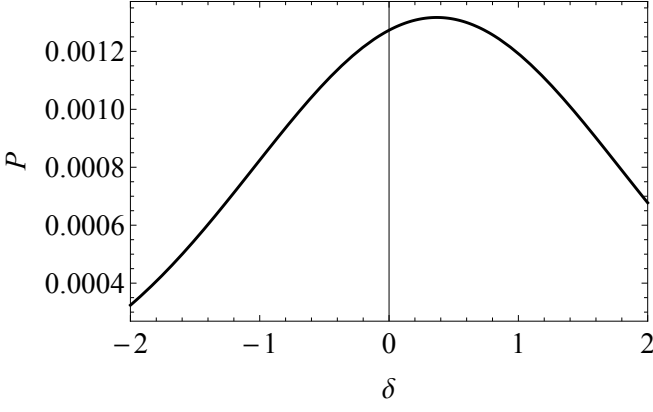


Figure 5. Probability,  $P(0.03, \delta)$ , for  $\eta = 10$ ,  $\epsilon = 0.001$ .

these sums are *distributions* that require regularization to converge, and these results are consistent with the results of Taylor [1].

This illustrates that the use of wavefunctions is essential for extracting the differential cross section using partial wave analysis.

Now we include the timing factor (101,102) and calculate the probability

$$P(\theta, \delta) = |\langle f | e^{-iHT} | i \rangle|^2, \quad (112)$$

given by (104). We find that the timing varies significantly with scattering angle. First we calculated the probability in the forward direction,  $\theta = 0$ , for  $\eta = 10$ , as a function of the spatial shift  $\delta$ . This showed a maximum at  $\delta = +1.2$ , corresponding to a time delay. We found later that the peak probability as a function of angle occurred at around  $\theta = 0.03$ . The profile in  $\delta$  for this angle is shown in Figure 5.

We find the maximum for this angle is at  $\delta = +0.4$ , corresponding to a time delay. In Section IX we will comment on the experimental measurability of this phenomenon.

Then we calculate the angular distribution,  $P(\theta, +0.4)$ , for this value of  $\delta$ , shown in Figure 6. For comparison we plot the Rutherford “probability”,

$$P_{\text{Ruth}}(\theta, \eta, \epsilon) = \frac{4\epsilon^4\eta^2}{\sin^4 \frac{\theta}{2}}, \quad (113)$$

which we obtain by naïvely converting the Rutherford differential cross section (2) into a probability using (85). Of course this is not a true probability since it rises above unity and diverges at  $\theta = 0$ .

We see deviation from the Rutherford formula for scattering angles less than about  $0.1 \text{ rad} = 5.7^\circ$ . There is also a shadow zone of low probability of angular width  $\sim 0.01 \text{ rad} = 0.6^\circ$  around the forward direction. In Section IX we will comment on the experimental measurability of this phenomenon.

We repeated this procedure for an attractive interaction ( $\eta = -10$ ) and found the profile in  $\delta$  for scattering

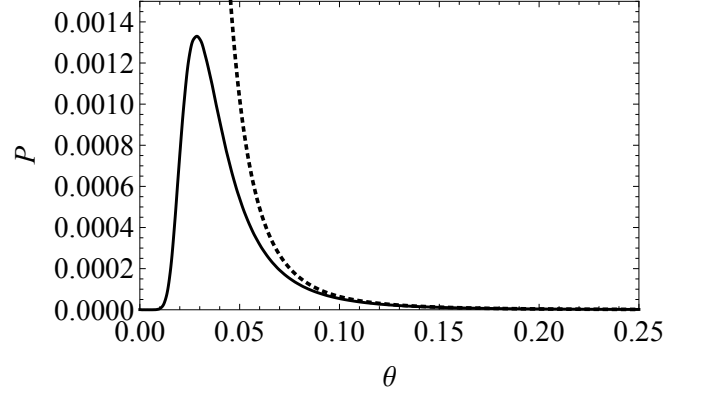


Figure 6. Probability  $P(\theta, +0.4)$  (solid) for  $\eta = 10$ ,  $\epsilon = 0.001$ , compared with  $P_{\text{Ruth}}$  (dotted).

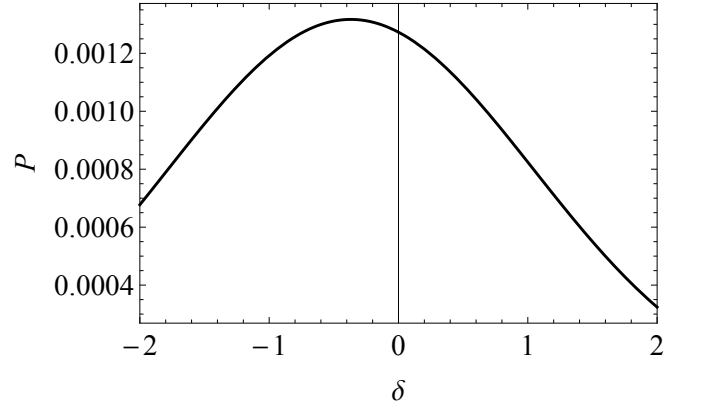


Figure 7. Probability  $P(0, \delta)$  for  $\eta = -10$  and  $\epsilon = 0.001$ .

angle  $\theta = 0.03$  shown in Figure 7. We see a peak at  $\delta = -0.4$ , corresponding to an advancement in time.

So we set  $\delta = -0.4$  and obtained the probability shown in Figure 8. The results are very similar to the case  $\eta = +10$ .

We considered a weaker interaction ( $\eta = 1$ ) with probability results shown in Figure 9. We see a strong forward peak and  $P(\theta, \delta)$  took its maximum at  $\delta \sim 0.05$ .

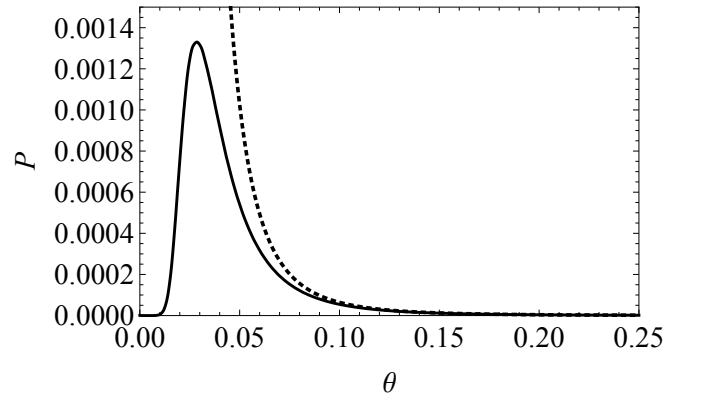


Figure 8. Probability,  $P(\theta, -0.4)$ , for  $\eta = -10$  and  $\epsilon = 0.001$ .

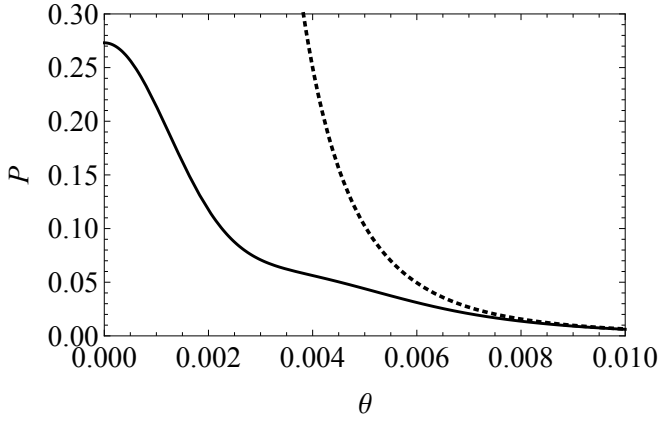


Figure 9. Probability,  $P(\theta, 0.05)$ , for  $\eta = 1$  and  $\epsilon = 0.001$ .

Boris et al. [5], in their visualizations of Coulomb scattering, saw shadow zones and interference fringes. However direct comparison with our results is not possible at present. As we will discuss later, we have chosen the simplest possible scattering geometry in this initial investigation, with vanishing impact parameter for our wavepackets. The wavepackets in Boris *et al.* [5] have nonzero impact parameters. We intend to explore the effects of nonzero impact parameters in a future work.

### VIII. CONSERVATION OF PROBABILITY

We can find a simple integral relation satisfied by the probabilities  $P(\theta, \delta)$  that expresses conservation of total probability. Starting from (112) and (104) and using the orthogonality of the Legendre polynomials and the integral

$$\frac{1}{\sqrt{4\pi}} \int_{-\infty}^{\infty} d\delta e^{-(\delta - \xi_l(p))^2/4} = 1, \quad (114)$$

it is easily shown that

$$\begin{aligned} \frac{1}{2\epsilon^2} \frac{1}{\sqrt{4\pi}} \int_{-\infty}^{\infty} d\delta \int_0^\pi \sin \theta d\theta P(\theta, \delta) = \\ 8\epsilon^2 \sum_{l=0}^{\infty} \left(l + \frac{1}{2}\right) e^{-4\epsilon^2(l + \frac{1}{2})^2} = 1 + \mathcal{O}(\epsilon^2). \end{aligned} \quad (115)$$

This relation holds for all interactions, including the free case with

$$P_{\text{Free}}(\theta, \delta) = e^{-\theta^2/4\epsilon^2} e^{-\delta^2/4}. \quad (116)$$

For non-Coulombic potentials (those that fall off with radial distance,  $r$ , faster than  $1/r$ ), the typical result is a strong forward peak ( $P \sim 1 - \mathcal{O}(\epsilon^2)$ ) and scattering at the  $\epsilon^4$  level. (These results will be presented in a future work.) So the forward peak dominates this integral. For the Coulomb cases  $\eta = \pm 10$ , we saw probabilities much larger than  $\mathcal{O}(\epsilon^4)$ , cut off at a finite value at a

small scattering angle and no forward peak. So these cases differ most dramatically from the expected form for non-Coulombic potentials. We would like to be confident that the total probability in our final states is unity. We ignored the  $\delta$  dependence and approximated the integral over  $\theta$  as a discrete sum with 200 points and found

$$\frac{1}{2\epsilon^2} \int_0^\pi \sin \theta d\theta P(\theta, 0.4) \cong 0.93. \quad (117)$$

We can use this integral relation to find an estimate of the angular size of the region where the Rutherford formula is violated. Suppose the probability factorized in the form

$$P(\theta, \delta) = e^{-(\delta - \delta_{\text{max}})^2/4} P(\theta), \quad (118)$$

which is a good approximation to the results we have been seeing. Then suppose the shadow region had vanishing probability on  $0 \leq \theta \leq \theta_0(\epsilon, \eta)$  and took the Rutherford form (113) at higher angles. Then we would have the integral relation

$$\frac{1}{2\epsilon^2} \int_{\theta_0}^\pi \sin \theta d\theta \frac{4\epsilon^4 \eta^2}{\sin^4 \frac{\theta}{2}} = 1. \quad (119)$$

For  $\epsilon\eta \ll 1$ , which includes the cases we have been considering, we find

$$\theta_0(\epsilon, \eta) \cong 4\epsilon|\eta|. \quad (120)$$

This gives  $\theta_0(0.001, \pm 10) \cong 0.04$  and  $\theta_0(0.001, 1) \cong 0.004$ . From Figures 7, 8 and 9, these estimates are seen to give good characterizations of the regions of violation.

### IX. MEASURABILITY OF THE PHENOMENA

Our numerical results have shown time delays along with shadow zones close to the forward direction. In an experiment well-described by Coulomb scattering, there must always be deviations from the Rutherford formula at low angles simply because the scattering probability cannot rise greater than unity. However a detector will always see a strong forward peak from events with sufficiently large impact parameters. The angular width of that forward peak may be such as to obscure the low-angle deviations.

The central problem in making contact with experiment is determining what momentum width,  $\sigma_p$ , should be used to describe the wavepackets emitted from the source of projectiles. We consider experiments similar to the original Geiger-Marsden experiments [17], in which alpha particles ( $Z_2 = +2$ ) were scattered by a thin gold foil (nuclei with  $Z_1 = +79$ ). The radioactive sources of alpha particles have very long half-lives. So the natural linewidths,  $\Delta E_N$ , as determined by the Heisenberg uncertainty principle, are extremely small. For Radium-226, with an emission at energy  $E = 4.8 \text{ MeV}$  of half-life 1600 years, this would give  $\epsilon = 6.8 \times 10^{-34}$ . If the

source is actually emitting wavepackets with this value of  $\epsilon$ , the observed differential cross section would be in complete agreement with the Rutherford formula down to extremely small angles.

The linewidths measured by magnetic spectroscopy with radioactive sources are much larger. Using extremely thin samples to reduce the scattering effects that broaden the linewidth, values as small as  $\Delta E = 2 \text{ keV}$  have been observed [18]. For the  $E = 4.8 \text{ MeV}$  emission of Radium-226, this would give  $\epsilon < 2.1 \times 10^{-4}$ , assuming that the actual energy width of the wavepacket could be smaller than the observed linewidth. For an experiment with these parameters, the strength parameter is  $\eta = 23.1$  and the estimated angle for deviation from Rutherford (from (120)) would be  $\theta_0 < 0.019 \text{ rad} = 1.1^\circ$ . This is significantly smaller than the typical angular width of the beam profile in a Rutherford experiment ( $\sim 5^\circ$  [19]), so the Rutherford deviation effects would be obscured. Note that to interpret the experiment, the predicted differential cross section must be convoluted with the beam profile.

There are experiments in which Helium nuclei are accelerated and directed towards nuclear targets [20]. It may be possible to achieve greater control over the wavepacket parameters in such an experiment.

The shift parameters,  $\delta_{\text{max}}$ , that we are seeing are of order unity. The corresponding time shifts are of order  $10^{-20} \text{ s}$ , certainly not measurable.

Wigner [21] reasoned that the spatial shift for  $l$ -wave scattering would be twice the derivative of the phase shift with respect to  $k$ . This is precisely what we have found, after taking into account the time shifts caused by the logarithmic phase. Wigner was considering in what way the classical concept of causality could be extended to the quantum domain, but his reasoning was based on the assumption of a potential of finite range.

We have chosen a particularly simple scattering geometry for this first investigation, as represented in Figure 2. In particular, the initial wavepacket approaches the center of the Coulomb potential head on, with no impact parameter. This geometry has been shown sufficient to extract a differential cross section. However, in the model experiment we are considering, the alpha particles would approach many gold nuclei with a continuous distribution of impact parameters. To predict the full scattering in the forward direction would require integrating probabilities over these impact parameters. We expect that a wavepacket with a sufficiently large impact parameter will pass the potential with minimal scattering. The

question of whether shadow zones remain after this integration will be investigated in a future work.

## X. CONCLUSIONS

The inclusion of wavepackets into the description of a scattering experiment does not merely smear the scattering amplitude. Instead, a rich variety of phenomena are predicted, including time shifts, a shadow zone and interference fringes. These phenomena are consistent with the view of a scattering process as the diffraction of a wave, in the appropriate parameter regime. We have presented predictions and examined the possibility of experimental observation.

From a theoretical perspective, we have shown that a wavepacket description allows the techniques of scattering theory, in particular partial wave analysis, to be applied to the long range Coulomb potential. We used a formalism that allowed treatment of the logarithmic phase in (47), a consequence of the infinite range of the Coulomb potential. This phase was shown to alter the long-distance trajectory of the wavepacket, in close agreement with the corresponding classical trajectory. We were able to extract the Rutherford differential cross section for scattering directions away from the forward direction. Around the forward direction, as in all directions, we calculated probabilities that were finite.

This method was made possible by the availability of the exact solutions for the energy angular momentum eigenfunctions. To apply the method to other central potentials would require the phase shifts for those potentials. Phase shifts have been calculated for the Yukawa [22], Morse [23] and spherical well potentials, for example. Note that Rawitscher *et al.* [23] calculated the motion of a wavepacket at a resonance. There are numerical methods available to calculate phase shifts in other cases [24].

The method could be extended to two-particle scattering by forming the eigenvectors of total energy, momentum and centre-of-mass frame angular momentum [25, 26]. Particles with spin are not an obstacle. If relativistic interactions are to be investigated, it is not widely known that there are relativistic probability amplitudes for particles of any spin, as discussed by Fong and Rowe [27]. For the electron, these are two-component rather than four-component objects.

- 
- [1] J. R. Taylor, *Il Nuovo Cimento B* (1971-1996) **23**, 313 (1974).
  - [2] K. Dettmann, *Zeitschrift für Physik* **244**, 86 (1971).
  - [3] H. Kröger and R. J. Slobodrian, *Phys. Rev. C* **30**, 1390 (1984).
  - [4] V. G. Baryshevskii, I. D. Feranchuk, and P. B. Kats,

*Phys. Rev. A* **70**, 052701 (2004).

- [5] S. D. Boris, S. Brandt, H. D. Dahmen, T. Stroh, and M. L. Larsen, *Phys. Rev. A* **48**, 2574 (1993).
- [6] J. D. Dollard, *Journal of Mathematical Physics* **5**, 729 (1964).
- [7] A. S. Kadyrov, I. Bray, A. M. Mukhamedzhanov, and

- A. T. Stelbovics, Phys. Rev. A **72**, 032712 (2005).
- [8] A. Kadyrov, I. Bray, A. Mukhamedzhanov, and A. Stelbovics, Annals of Physics **324**, 1516 (2009), july 2009 Special Issue.
- [9] A. Messiah, *Quantum Mechanics*, Vol. 1 and 2 (North-Holland, Amsterdam and John Wiley and Sons, N.Y., 1961).
- [10] E. Merzbacher, *Quantum Mechanics*, 3rd ed. (John Wiley and Sons, Inc., 1998).
- [11] E. Rutherford, Philosophical Magazine **Series 6**, vol. **21** (1911).
- [12] J. J. Sakurai, *Modern Quantum Mechanics*, revised edition ed. (Addison-Wesley, Reading, MA, 1994).
- [13] S. E. Hoffmann, Paper in preparation (2017).
- [14] I. S. Gradshteyn and I. M. Ryzhik, *Tables of Integrals, Series and Products*, corrected and enlarged ed. (Academic Press, Inc., San Diego, CA, 1980).
- [15] R. G. Newton, *Scattering theory of waves and particles*, 2nd ed. (Springer-Verlag, N.Y., 1982).
- [16] E. H. Wichmann, American Journal of Physics **33**, 20 (1965).
- [17] H. Geiger and E. Marsden, Proc. Roy. Soc. **82**, 495 (1909).
- [18] S. Pommé, Metrologia **52**, S146 (2015).
- [19] T. H. Kim, Private communication (2008).
- [20] R. A. Anokhin, V. N. Voyevodin, S. N. Dubnyuk, A. M. Egorov, B. V. Zaitsev, A. F. Kobets, O. P. Ledenyov, K. V. Pavliy, V. V. Ruzhitsky, and G. D. Tolstolutskaia, <https://arXiv.org/pdf/1309.2523.pdf> (2013).
- [21] E. P. Wigner, Phys. Rev. **98**, 145 (1955).
- [22] M. Hamzavi, M. Movahedi, K.-E. Thylwe, and A. A. Rajabi, Chinese Physics Letters **29**, 080302 (2012).
- [23] G. Rawitscher, C. Merow, M. Nguyen, and I. Simbotin, American Journal of Physics **70**, 935 (2002).
- [24] J. P. Klozenberg, Journal of Physics A: Mathematical, Nuclear and General **7**, 1840 (1974).
- [25] M. Jacob and G. C. Wick, Annals of Physics (N.Y.) **7**, 404 (1959).
- [26] A. J. Macfarlane, Rev. Mod. Phys. **34**, 41 (1962).
- [27] R. Fong and E. Rowe, Annals of Physics **46**, 559 (1968).

## ACKNOWLEDGMENTS

The author is grateful to Diane and Lydia and to his mother, Mark, Adam and their families for their love and support. The author is also grateful to Anwen King for helpful discussions, and to Yao-Zhong Zhang and Ian Marquette for their support.